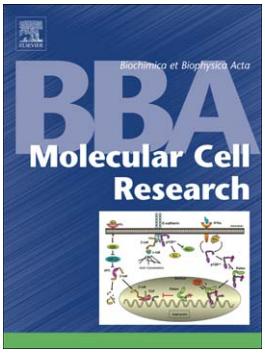

Molecular characterization of human osteoblast-derived extracellular vesicle mRNA using next-generation sequencing

Jess Morhayim, Jeroen van de Peppel, Amel Dudakovic, Hideki Chiba, Andre J. van Wijnen, Johannes P. van Leeuwen

PII: S0167-4889(17)30065-4
DOI: doi:10.1016/j.bbamcr.2017.03.011
Reference: BBAMCR 18067

To appear in: *BBA - Molecular Cell Research*

Received date: 20 October 2016
Revised date: 27 February 2017
Accepted date: 23 March 2017

Please cite this article as: Jess Morhayim, Jeroen van de Peppel, Amel Dudakovic, Hideki Chiba, Andre J. van Wijnen, Johannes P. van Leeuwen, Molecular characterization of human osteoblast-derived extracellular vesicle mRNA using next-generation sequencing, *BBA - Molecular Cell Research* (2017), doi:10.1016/j.bbamcr.2017.03.011

Molecular characterization of human osteoblast-derived extracellular vesicle mRNA using next-generation sequencing

Jess Morhayim[a], Jeroen van de Peppel[a], Amel Dudakovic[b], Hideki Chiba[c], Andre J. van Wijnen[b] and Johannes P. van Leeuwen[a,*]

[a]Department of Internal Medicine, Erasmus Medical Center, Wytemaweg 80, 3015 CN, Rotterdam, the Netherlands; j.morhayim@erasmusmc.nl

[a]Department of Internal Medicine, Erasmus Medical Center, Wytemaweg 80, 3015 CN, Rotterdam, the Netherlands; h.vandepeppel@erasmusmc.nl

[b]Department of Orthopedic Surgery, Mayo Clinic, Rochester, MN, USA; dudakovic.amel@mayo.edu

[c]Fukushima Medical University School of Medicine, Hikarigaoka, 960-1295, Fukushima, Japan; hidchiba@fmu.ac.jp

[b]Department of Orthopedic Surgery, Mayo Clinic, Rochester, MN, USA; vanwijnen.andre@mayo.edu

[a]Department of Internal Medicine, Erasmus Medical Center, Wytemaweg 80, 3015 CN, Rotterdam, the Netherlands; j.vanleeuwen@erasmusmc.nl

* To whom correspondence should be addressed. Tel: +31(10)7033405; Fax: +31(10)7032603; Email: j.vanleeuwen@erasmusmc.nl

ABSTRACT

Extracellular vesicles (EVs) are membrane-bound intercellular communication vehicles that transport proteins, lipids and nucleic acids with regulatory capacity between cells. RNA profiling using microarrays and sequencing technologies has revolutionized the discovery of EV-RNA content, which is crucial to understand the molecular mechanism of EV function. Recent studies have indicated that EVs are enriched with specific RNAs compared to the originating cells suggestive of an active sorting mechanism. Here, we present the comparative transcriptome analysis of human osteoblasts and their corresponding EVs using next-generation sequencing. We demonstrate that osteoblast-EVs are specifically depleted of cellular mRNAs that encode proteins involved in basic cellular activities, such as cytoskeletal functions, cell survival and apoptosis. In contrast, EVs are significantly enriched with 254 mRNAs that are associated with protein translation and RNA processing. Moreover, mRNAs enriched in EVs encode proteins important for communication with the neighboring cells, in particular with osteoclasts, adipocytes and hematopoietic stem cells. These findings provide the foundation for understanding the molecular mechanism and function of EV-mediated interactions between osteoblasts and the surrounding bone microenvironment.

Keywords: Extracellular vesicles; Intercellular communication; Osteoblasts; Extracellular mRNA; Next-generation sequencing

Abbreviations:

EV: Extracellular vesicles

1. Introduction

Extracellular RNAs have long been utilized as non-invasive tools for early diagnosis of clinical disorders [1, 2]. More recently, various studies reported RNA transfer between cells providing cues to their biological significance [3, 4]. The majority of extracellular RNA is found in tight complexes with proteins or lipids, as a protection against the action of RNases present in the circulation [5, 6]. The discovery of extracellular RNA with regulatory capacity packaged inside extracellular vesicles (EVs) provided a key indication for EVs as a novel mode of communication between cells [7-9].

EVs are actively secreted small membrane-bound structures consisting of a lipid bilayer enclosing a lumen that contains a bioactive message in forms of lipids, proteins and nucleic acids [10-12]. Extensive studies of EVs present in cell culture media or biological fluids revealed that EVs are very heterogeneous in size (10 nm to 5 μm) and morphology. Most often they are classified in at least three categories, such as exosomes, microvesicles and apoptotic bodies, merely based on their biogenesis. Their specific structure is essential for the protection of the vesicular cargo in the extracellular environment until they reach the target cells, where they regulate a broad range of biological functions [13-15]. Advanced high throughput RNA and protein analysis methods (‘omics’ technologies) have greatly facilitated the characterization of EV content and our ability to understand EV function. Since the first discovery of

EV-associated RNA, many studies have focused on delineating the EV-RNA profile [16-18]. Interestingly, EVs are devoid of cellular ribosomal RNA (rRNA), and instead are enriched with small RNA molecules. This selective enrichment of RNA species suggests that RNA enters EV through active sorting rather than random incorporation as a by-product of cell death [8]. Moreover, distinct EV-RNA patterns are evident in EVs from different cellular sources emphasizing the specificity of cargo loading in EVs. Expression profiling studies focusing on mRNA and microRNA (miRNA) analysis by next-generation sequencing or microarray analyses have shown that numerous small non-coding RNA molecules (e.g. small nuclear RNAs, vault RNA, Y RNA) are present inside EVs [19-21]. At present, there is a significant body of evidence indicating that EV-RNAs are important for development, immunology, angiogenesis, stem cell biology, and cancer, among many other biological functions [22-25].

Osteoblasts are specialized bone cells that are responsible for the formation of mineralized bone tissue. Yet, these cells also play pivotal roles in maintaining cellular homeostasis by regulating interactions with surrounding cells [26-28]. Previously, we showed that osteoblasts secrete EVs packaged with functional proteins that contribute to the complex network of communication with the cells in the osteoblastic microenvironment [29]. The crosstalk is also highly regulated at the level of gene expression. In the present study, we employed next-generation sequencing analysis for in-depth characterization of the mRNA content of EVs that are secreted by human osteoblasts. Using a bioinformatics workflow, we described mRNA species that are

selectively incorporated into EVs or depleted from EVs during their biogenesis, and explored the molecular functions by which osteoblasts may deliver their specific regulatory message. Our comprehensive transcriptome profiling represents a versatile resource for diverse biomedical applications ranging from biomarker discovery to gene therapy.

2. Materials and methods

2.1. Cell culture and EV isolation

Simian virus 40-immortalized human osteoblast cells (SV-HFO cells) were cultured under non-mineralizing conditions in α-MEM (GIBCO, Paisley, UK) supplemented with 20 mM HEPES, pH 7.5 (Sigma, St. Louis, MO, USA), streptomycin/ penicillin, 1.8 mM $CaCl_2$ (Sigma), 10 mM β-glycerophosphate (Sigma) and 2% depleted (100,000g for 90 minutes at 4°C)-FCS (GIBCO) at 37°C in a humidified atmosphere of 5% CO_2 for 14 days. The culture medium was replaced every 2-3 days. SV-HFOs were washed with 1X PBS and refreshed with serum-free medium 24 hours prior to EV isolation. EVs were isolated from SV-HFO conditioned medium by low speed centrifugation (1,500 rpm, 5 minutes; 4,500 rpm, 10 minutes) followed by ultracentrifugation (20,000g, 30 minutes; 100,000g, 1 hour at 4°C) using the SW32Ti rotor (Beckman Coulter, Fullerton, CA, USA).

2.2. RNA isolation and quantitative real-time PCR

Total cellular and EV-RNA was isolated using the TRIzol® reagent (Thermo Fisher Scientific, Waltham, MA, USA) according to the manufacturer's instructions. RNA concentration was determined using Nanodrop (Thermo Fisher Scientific) and size distribution was checked on an Agilent Bioanalyzer RNA 6000 Nano chip (Thermo Fisher Scientific). Quantitative real-time PCR was performed using the SYBR™ Green kit (Eurogentec, Seraing, Belgium) according to the manufacturer's instructions. The primer sequences are listed in supplementary information.

2.3. Next-generation sequencing and bioinformatics analysis

RNA sequencing and bioinformatic analysis was performed as previously described [30]. In brief, sequencing RNA libraries were prepared with the TruSeq RNA Sample Prep Kit v2 (Illumina, San Diego, CA, USA) according to the manufacturer's instructions. The concentration and size distribution of the libraries was determined on an Agilent Bioanalyzer DNA 1000 chip (Thermo Fisher Scientific), and verified with Qubit fluorometry (Thermo Fisher Scientific). Libraries were loaded onto flow cells at concentrations of 8–10 pM to generate cluster densities of 700,000/ mm^2 following the standard protocol for the Illumina cBot and cBot Paired-end cluster kit version 3. Flow cells were sequenced as 51 × 2 paired end reads on an Illumina HiSeq

2000 using TruSeq SBS sequencing kit version 3 and HCS v2.0.12 data collection software. Base-calling was performed using Illumina's RTA version 1.17.21.3. The sequencing data are available in the Gene Expression Omnibus **(**GEO**)** database repository (https://www.ncbi.nlm.nih.gov/geo/) under accession number GSE85761. The sequencing data was analyzed using MAPRSeq v1.2.1 system. Normalization (counts per million mapped reads, CPM; and reads per kilobasepair per million mapped reads, RPKM) analysis was performed using edgeR 2.6.2. The data from the replicates were combined as averages of the normalized read values, and only transcripts with CPM ≥ 1 for all replicates were included in the analysis. Comparative analyses of the EV data were obtained by querying the Vesiclepedia plugin provided by FunRich functional enrichment analysis tool (V2.1.2, 29 April 2015). IPA (Ingenuity® Systems, www.ingenuity.com) was used to classify the mRNA categories and predict target pathways and genes. DAVID Bionformatics Resources v6.7 was used to categorize the genes into overrepresented processes using human genome as a background [31].

2.4. Statistics

The data provided were based on multiple independent experiments. The results were described as mean ± SD. Significance was calculated using paired Student's *t*-test, and *P* values of < 0.05 were considered significant.

3. Results

3.1. Osteoblasts secrete RNA containing EVs

To characterize the transcriptome of EVs, we isolated RNAs present in EVs released by human osteoblastic cells (SV-HFOs) at day 12-14 of their maturation. We isolated EVs using a step-wise differential ultracentrifugation protocol, and isolated total EV-RNA using the TRIzol® extraction method. Quality control of RNA samples revealed that the yield is consistent between the independent EV preparations, with an average of 2.6 µg EV-RNA deriving from 80 ml of culture medium. In parallel, we also isolated total RNA from the same osteoblasts to permit a direct comparison of RNA content. Representative Bioanalyzer electropherograms show expected differences in the RNA size distribution profiles for osteoblasts and their corresponding EVs (Fig. 1a,b). EVs mainly contain small RNAs with a size range between 25 and 1,000 nucleotides, and lack the intact rRNA peaks characteristic of cellular 18S and 28S rRNAs. These findings emphasize the robustness of our isolation techniques and clearly demonstrate the distinctiveness of EV-RNA content compared to their parental cells.

3.2. EV-mRNA profiling using next-generation sequencing

We investigated the EV-mRNA profile at high resolution by next-generation sequencing. We constructed sequencing libraries from three independent osteoblast cultures and their derived EVs, and analyzed the data using an established bioinformatics workflow (Fig. 2).

The detected RNA read counts are robust and reproducible between the sequencing libraries, indicating a consistent distribution across independent preparations (Supplementary Table 1). Scatter plot analysis shows a fairly strong positive correlation between cellular RNA and EV-RNA (R^2: 0.731, $P < 0.0001$) (Fig. 3a). The majority of the sequencing reads are mapped to mRNA sequences for both osteoblasts (11,714 mRNAs) and EVs (11,629 mRNAs) (Fig. 3b). Classification of cellular- and EV-mRNAs shows a high diversity of biochemical functions (Fig. 3c).

As it is evident from the scatter plot, the majority of the mRNAs are shared between osteoblasts and EVs. Yet, a small but significant fraction of mRNAs is exclusive to either osteoblasts or EVs [5.9% (693 mRNAs) and 5.2% (608 mRNAs), respectively] (Fig. 4a). These exclusive mRNAs are expressed at relatively low levels and represent a small fraction of total cellular- and EV-mRNA read counts (0.16% and 0.17%, respectively).

Interestingly, the top 100 highly expressed genes account for 58.25% of all mapped EV-mRNA read counts, whereas only 34.04% account for the top 100 mapped mRNAs in the cells (Fig. 4b). This result suggests a specific enrichment of biologically significant mRNAs in EVs. The majority of these mRNAs (78 mRNAs) appear in both the top 100 of either the cellular- or EV-derived transcriptome, and many encode rather ubiquitous ribosomal proteins (Fig. 4c). The remaining top EV-mRNAs (22 mRNAs) are mostly associated with oxidative phosphorylation and protein transport (Fig. 4d). In contrast, the cellular transcriptome is enriched with mRNAs required for essential cellular functions, such as glycolysis, cell motion and regulation of apoptosis (Fig. 4e). Taken together, these results indicate that even though EV-mRNA content mirrors the transcriptome of their donor cells, EVs exhibit a distinct pattern in distribution of mRNA abundance. These findings clearly indicate that mRNAs are selectively sorted into EVs, rather than randomly incorporated during vesicular trafficking and extracellular release.

3.3. EVs are selectively enriched with a subset of mRNAs

We assessed the relative abundance of mRNAs in cells and EVs to determine the types of mRNAs that are specifically enriched in EVs. Volcano plotting shows that 254 mRNAs are significantly ($P < 0.05$) more abundant (≥ two-fold) in EVs compared to the cells (Fig. 5a, Supplementary Table 2). The most highly enriched

EV-mRNAs ("Top 10") are *RAB13*, *ARRDC4*, *NEFM*, *IGIP*, *NET1*, *RASSF3*, *HMGN5*, *TRAK2*, *ESF1* and *ZEB1*, in descending order of fold enrichment.

Bioinformatic analysis using the Ingenuity Pathway Analysis (IPA) revealed that cellular processes, such as RNA post-transcriptional modification, gene expression and cell-to-cell signaling and interaction, are strongly overrepresented in EV-mRNAs. On the other hand, the transcriptome of EVs is depleted of 2,192 cellular mRNAs that are selectively linked to essential cellular processes, such as cell death and survival and cellular growth and proliferation. Gene Ontology (GO) enrichment analyses demonstrate the specific depletion of organelle-specific (i.e. endoplasmic reticulum, Golgi apparatus, endosome) mRNAs from EVs suggesting a functional role not primarily linked to intracellular trafficking (Supplementary Fig. S1). On the other hand, based on IPA analysis EVs preferentially contain mRNAs that encode proteins involved in cell-to-cell communication in the bone and bone marrow microenvironment. These include the genes involved in the recruitment of osteoclasts (*NFKBIB*, *PGF*), priming of adipose cells (*FGF1*), as well as self-renewal and proliferative expansion of hematopoietic stem and progenitor cells (*FLT3LG*, *IL18*, *HOXB7*, *CCND1*, *CCND2*) (Fig. 5b).

Among the 254 enriched EV-mRNAs, osteoblast-EVs contain 49 unique mRNAs that have not been previously detected in EVs secreted by other cells or present in body fluids (Fig. 5c) [32]. These novel mRNAs have gene ontology annotations related to zinc ion-binding (*AGAP2*, *ZNF677*, *ZNF846*), regulation of

transcription (*BDP1*, *SOX11*, *TAF7L*) and kinase activity (*LPAR1*, *MAP3K13*, *ZEB2*). Furthermore, we compared the enriched EV-mRNA dataset to the previously characterized protein content of these EVs [29]. For a limited number of mRNAs (18 mRNAs), osteoblast-EVs contain the corresponding protein (Fig. 5d). Two of these are derived from osteoblast-EV specific mRNAs (*HIST1H1E* and *LPAR1*), whereas the remaining 16 proteins include ribonucleoproteins (*HNRNPA1*, *HNRNPA3*, *HNRNPH3*), translation initiation factors (*EIF3A*, *EIF5B*), histones (*HIST1H2BH*, *HIST1H2BO*) and others (*MAP4K4*, *NAP1L1*, *NCL*, *PABPC1*, *RAB13*, *SEPT7*, *SET*, *ST13*, *YES1*). It is important to note that all the exons are covered by significant reads for the majority of the EV-mRNAs, confirming the enrichment of full-length mRNAs inside EVs (Fig. 6a). 169 out of 254 enriched EV-mRNAs demonstrate full (100%) exon coverage, while only 33 mRNAs have less than 50% coverage. Read coverage is uniform across the exons of the highly abundant mRNAs overrepresented in EVs (Fig. 6b-e, Supplementary Fig. S2). Furthermore, the majority of the full-length enriched EV-mRNAs are of intermediate size (100 – 500 bp) (Fig. 6f).

Next, we visualized log ratios of the normalized read counts for mRNAs from EVs versus cells relative to their mean abundance. The resulting MA plot compares the expression levels of the 254 mRNAs enriched by at least two-fold in EVs. Remarkably, *RAB13* is both the most highly enriched and most abundant EV-mRNA that is selectively incorporated in EVs compared to the EV-producing osteoblasts (Fig. 7a). Furthermore, it is the only member of the Rab GTPase family with such a striking selective abundance in EVs, strongly suggesting that *RAB13* is specifically

enriched in EVs (Fig. 7b). We evaluated the expression levels of *RAB13* along with *ATP5E*, which shows similar cellular and vesicular abundances in sequencing analysis (Fig. 7c). Quantitative real-time PCR results confirm the significant enrichment of *RAB13* in EVs, consistent with the sequencing data (Fig. 7d). Using IPA, we investigated the molecular functions and canonical pathways associated with the RAB13 protein (Fig. 7e). We identified 26 proteins that are directly or indirectly coupled to the activity of RAB13. These proteins have molecular and cellular functions related to DNA replication, recombination and repair, cellular growth and proliferation, cellular assembly and organization, cell movement, and cell morphology. The main canonical pathways in which RAB13 participates are TGF-β signaling, cell cycle control of chromosomal replication and nucleotide excision repair pathway. In addition, several of these RAB13 associated proteins regulate the proliferation of stromal cells, chondrocytes, blood cells and tumor cells, which are precisely the potential target cells that physiologically interact with osteoblasts in the bone microenvironment. Taken together, our study is consistent with the broader concept that osteoblasts communicate with their surrounding cells by generating EVs that are actively loaded with specific bioactive molecules. This molecular cargo encompasses a selective group of mRNAs capable of providing defined regulatory signals to recipient cells.

4. Discussion

The discovery of extracellular RNA (e.g. circulating RNA, EV-RNA) with regulatory functions has tremendous ramifications for both medical sciences and clinical applications. In this study, we reported the extensive profiling of mRNAs incorporated within EVs released by human osteoblasts. We showed that EVs to some degree contain the mRNA signature of their host cells while being selectively enriched with a unique set of mRNAs that may support intercellular communication. Our findings provide a major advancement in our understanding of EVs as a newly discovered mode of communication between osteoblasts and the surrounding microenvironment.

We previously showed that osteoblasts secrete EVs containing a specific set of proteins important for their communication with their target cells [29]. Here, we investigated the mRNA profile of osteoblast-EVs to further characterize and discover the role of EVs in intercellular communication. Currently, the EV field is still challenged by variation in the reliability and procedural differences in EV-RNA isolation protocols [33, 34]. In our study, we reproducibly obtained satisfactory RNA yields with robust size distributions that were consistent between the different preparations. Bioanalyzer profiles of our total RNA preparations show that osteoblast-EVs lack the typical cellular rRNAs and are enriched with small RNAs that range from 25 to 1,000 nucleotides, in accordance with other EV-RNA studies [35-37].

Diverse cell types secrete small EV-RNAs that mainly consist of miRNAs and other small non-coding RNA molecules. Yet, there is increasing evidence showing the presence of functional mRNA specifically packaged inside EVs. However, intact mammalian mRNAs typically range between 400 and 12,000 nucleotides in length [38]. The smaller size range of osteoblast-EV-derived RNAs inevitably leads to the question whether EVs merely contain mRNA fragments. A report by Batagov and colleagues presented data indicating that EVs contain fragments derived from the 3'-untranslated regions (3'-UTR) of certain mRNAs to protect the target mRNA against miRNA degradation [39]. On the other hand, our exon coverage analyses demonstrate that osteoblast-EVs are specifically enriched with full-length mRNAs of intermediate size. Several other studies reported the transfer of full-length EV-mRNA between cells with subsequent translation into functional proteins by the recipient cells [40-42]. It is conceivable that cells may transmit both full-length mRNAs and 3'-UTR fragments as a two-pronged strategy that, first, instructs translation of proteins in the recipient cell, and second, relieves miRNA-mediated translation inhibition by competition with 3'-UTRs containing relevant miRNA binding sequences.

Next-generation sequencing technologies have permitted comprehensive analyses of whole transcriptomes with single nucleotide resolution and quantitative assessments of RNA levels. We applied next-generation sequencing to identify RNA reads that correspond to 11,629 EV-mRNAs. The content and abundance profile of this mRNA set mirrors the mRNAs detected in donor cells. Because EVs may form by budding from the plasma membrane or exocytosis of multivesicular bodies, it is

possible that cellular components are non-specifically incorporated into EVs during their biogenesis. Indeed, many mRNAs present in EVs are similarly abundant in the cells that produce them suggesting that they are simply stochastically distributed into EVs. For example, mRNAs for ribosomal proteins are highly abundant in cells and also found in top 100 in EV-mRNAs. Nevertheless, there are a number of mRNAs that are either selectively enriched or depleted in EVs compared to the producing cells. The quantitative and qualitative differences in the transcriptome of EVs versus cells clearly suggest that at least some mRNAs may be specifically sorted and packaged into EVs to support cell–cell communication.

Comparative transcriptome analyses reveal selective enrichment and depletion of particular mRNAs that are significantly overrepresented (254 mRNAs) or underrepresented (2,193 mRNAs) in EVs when compared to the producing cells. EVs appear to be specifically depleted of mRNAs required for vital cellular functions, yet many enriched EV-mRNAs encode proteins that directly or indirectly mediate mRNA translation by supporting the biogenesis of ribosomes (e.g., enzymes that mediate rRNA processing or structural ribosomal proteins). Because 18S and 28S rRNAs, which are two major constituents of the ribosome, are not detected in the total RNA distribution of EVs compared to that of cells and the abundance of mRNAs encoding a particular subset of ribosomal proteins may suggest a specific role in vesicular function. Consistent with our findings, previous studies reported that EVs contain mRNAs encoding ribosomal proteins, as well as elongation and translation factors [8, 43]. Furthermore, Jenjaroenpun and colleagues suggested that these genes upon

translation in the recipient cells may provide essential ribosomal components to support the translation of other EV-mRNAs [44]. Previously, we showed that the stages of differentiation and the mineralization condition are also among the factors that influence the nature and abundance of EV cargo [29]. EVs secreted by mineralizing osteoblasts are enriched with biomineralization-related proteins indicating an activity associated with bone formation. On the other hand, the enrichment of ribosomal proteins as well as mRNAs that encode ribosomal proteins in EVs secreted by non-mineralizing osteoblasts brings diverse speculations on their role of stabilizing the miRNA cargo or transferring of ribosomal parts to facilitate gene expression in the target cells. At this stage, it is still challenging to distinguish the role of individual EV cargo. In light of our findings, we can conclude that regardless of the possibility that EV-mRNAs may be involved in very common cellular activities, the most interesting mRNA species are those that are less abundant, as well as fairly unique to EVs and not represented in the recipient cell.

Crosstalk between osteoblasts and the surrounding bone microenvironment is critical to maintain essential biological processes, such as osteoclastogenesis, hematopoiesis and adipogenesis. Hence, a major objective of our studies is to identify unique mRNAs in EVs that could affect the biological state of the recipient cell. The majority of the mRNAs enriched in osteoblast-EVs are also detected in EV preparations from other cells and body fluids, suggesting that some of these mRNAs may have common functions related to generic activities of EVs, rather than specific biological roles linked to the bone microenvironment. However, a substantial subset

(~20%) of the enriched mRNAs is uniquely detected in osteoblast-EVs and thus can be attributed to a specific osteoblast-related and EV-mediated function. Enriched osteoblast-EV-mRNAs include those that encode proteins capable of regulating the fate of target neighboring cells in the bone microenvironment. Therefore, it is intriguing that such regulatory mRNAs are selectively sorted into osteoblast-EVs. We anticipate that further investigation of EV-specific mRNAs will permit delineation of the EV-mediated mechanisms by which osteoblasts communicate and control an intricate cell-to-cell interaction network in the bone microenvironment.

The most strikingly overrepresented EV-mRNA is *RAB13*, because it is exceptionally abundant in EVs compared to the cells. RAB13 protein is a member of the Rab family of small GTPases, which are primarily involved in vesicle trafficking, including vesicle production and fusion at the target cell membrane [45]. Furthermore, even though our studies yielded very few examples in which mRNAs and their encoded proteins are co-packaged in EVs, osteoblasts-EVs not only contain *RAB13* mRNA but also the RAB13 protein. RAB13 protein may have a role in EV biogenesis and cargo sorting at the donor cell membrane [29]. However, the enrichment of this mRNA in osteoblast-EVs and its putative transfer into recipient cells could represent a regulatory mechanism by which osteoblasts control EV production in their target cells. Beyond the latter possibility, Rab proteins also regulate cytoskeleton organization and assembly of tight junctions, and thereby regulate cell adhesion necessary for cell growth [46, 47]. Accordingly, our network analysis predicted potential RAB13 targets that play important roles in the

proliferation of chondrocytes, stromal, blood and tumor cells, indicative of a possible role in communication between osteoblasts and the target cells within the bone microenvironment.

Osteoblasts are known to communicate with osteoclasts to coordinate tissue mineralization and resorption during bone remodeling. Intriguingly, Rab family proteins have essential roles in osteoclastic membrane trafficking required for bone resorption [48, 49]. RAB13, in particular, has been shown to be upregulated during osteoclast differentiation where it engages in vesicular trafficking events unrelated to bone resorption [50]. The possibility arises that osteoblasts could deliver RAB13 to immature osteoclasts via EVs to alter the osteoclast phenotype and perhaps provoke secondary extracellular signals emanating from osteoclasts. A number of follow-up studies will be required to identify potential target cells of osteoblast-EVs, establish how EVs unload their cargo and determine how EVs affect the biological properties of recipient cells.

In conclusion, in this study we present a comprehensive analysis of the EV transcriptome that suggests new mechanistic concepts. Our studies suggests a model in which EVs produced by osteoblasts may be part of a paracrine signaling system that coordinates the biological functions of both skeletal and hematopoietic cells in the bone microenvironment. Our results provide the molecular basis for understanding the biological significance of EV-mRNAs in the context of bone related processes. It remains to be elucidated whether EV-mRNAs are translated and consequently are

rendered functional upon delivery into the target cells. Finally, EV transcriptome-profiling offers a potent avenue for discovery of non-invasive diagnostics for various diseases and facilitates the development of cell-free strategies for regenerative therapy.

Funding

This work was supported by a grant from the Dutch government to the Netherlands Institute for Regenerative Medicine (grant number FES0908 to JPvL), Erasmus MC Stem Cell and Regenerative Medicine Institute and Erasmus University Medical Center. Additional support was provided by the US National Institutes of Health grants (grant numbers R01-AR049069 to AJvW, F32-AR066508 to AD). Funding for open access charge: Netherlands Institute for Regenerative Medicine.

Acknowledgements

We thank Jared Evans and Asha Nair at Mayo Clinic for assistance with bioinformatic analysis of high-throughput mRNA sequencing. We also appreciate the support of other laboratory members and collaborators, including Bram van der Eerden, Roman Thaler, Alfonso Eirin and Lilach Lerman, for stimulating discussions and/or sharing of unpublished data.

References

[1] A.J. Wieczorek, V. Sitaramam, W. Machleidt, K. Rhyner, A.P. Perruchoud, L.H. Block, Diagnostic and prognostic value of RNA-proteolipid in sera of patients with malignant disorders following therapy: first clinical evaluation of a novel tumor marker, Cancer research, 47 (1987) 6407-6412.

[2] M.S. Kopreski, F.A. Benko, L.W. Kwak, C.D. Gocke, Detection of tumor messenger RNA in the serum of patients with malignant melanoma, Clinical cancer research : an official journal of the American Association for Cancer Research, 5 (1999) 1961-1965.

[3] G.M. Kolodny, Evidence for transfer of macromolecular RNA between mammalian cells in culture, Experimental cell research, 65 (1971) 313-324.

[4] P. Galand, L. Ledoux, Uptake of exogenous ribonucleic acid by ascites tumor cells. II. Relations between RNA uptake and the cellular metabolism, Experimental cell research, 43 (1966) 391-397.

[5] J.D. Arroyo, J.R. Chevillet, E.M. Kroh, I.K. Ruf, C.C. Pritchard, D.F. Gibson, P.S. Mitchell, C.F. Bennett, E.L. Pogosova-Agadjanyan, D.L. Stirewalt, J.F. Tait, M.

Tewari, Argonaute2 complexes carry a population of circulating microRNAs independent of vesicles in human plasma, Proceedings of the National Academy of Sciences of the United States of America, 108 (2011) 5003-5008.

[6] M. Fleischhacker, Biology of circulating mRNA: still more questions than answers?, Annals of the New York Academy of Sciences, 1075 (2006) 40-49.

[7] M. Ceccarini, L. Guidoni, A.M. Luciani, G. Mariutti, A. Rosi, V. Viti, Biochemical and NMR studies on structure and release conditions of RNA-containing vesicles shed by human colon adenocarcinoma cells, International journal of cancer. Journal international du cancer, 44 (1989) 714-721.

[8] H. Valadi, K. Ekstrom, A. Bossios, M. Sjostrand, J.J. Lee, J.O. Lotvall, Exosome-mediated transfer of mRNAs and microRNAs is a novel mechanism of genetic exchange between cells, Nature cell biology, 9 (2007) 654-659.

[9] A. Montecalvo, A.T. Larregina, W.J. Shufesky, D.B. Stolz, M.L. Sullivan, J.M. Karlsson, C.J. Baty, G.A. Gibson, G. Erdos, Z. Wang, J. Milosevic, O.A. Tkacheva, S.J. Divito, R. Jordan, J. Lyons-Weiler, S.C. Watkins, A.E. Morelli, Mechanism of transfer of functional microRNAs between mouse dendritic cells via exosomes, Blood, 119 (2012) 756-766.

[10] C. Thery, M. Ostrowski, E. Segura, Membrane vesicles as conveyors of immune responses, Nat Rev Immunol, 9 (2009) 581-593.

[11] D.A. Shifrin, Jr., M. Demory Beckler, R.J. Coffey, M.J. Tyska, Extracellular vesicles: communication, coercion, and conditioning, Mol Biol Cell, 24 (2013) 1253-1259.

[12] J. Morhayim, M. Baroncelli, J.P. van Leeuwen, Extracellular vesicles: specialized bone messengers, Archives of biochemistry and biophysics, 561 (2014) 38-45.

[13] E. Cocucci, G. Racchetti, J. Meldolesi, Shedding microvesicles: artefacts no more, Trends Cell Biol, 19 (2009) 43-51.

[14] B. Gyorgy, T.G. Szabo, M. Pasztoi, Z. Pal, P. Misjak, B. Aradi, V. Laszlo, E. Pallinger, E. Pap, A. Kittel, G. Nagy, A. Falus, E.I. Buzas, Membrane vesicles, current state-of-the-art: emerging role of extracellular vesicles, Cell Mol Life Sci, 68 (2011) 2667-2688.

[15] G. Raposo, W. Stoorvogel, Extracellular vesicles: exosomes, microvesicles, and friends, J Cell Biol, 200 (2013) 373-383.

[16] S.A. Bellingham, B.M. Coleman, A.F. Hill, Small RNA deep sequencing reveals a distinct miRNA signature released in exosomes from prion-infected neuronal cells, Nucleic Acids Res, 40 (2012) 10937-10949.

[17] X. Huang, T. Yuan, M. Tschannen, Z. Sun, H. Jacob, M. Du, M. Liang, R.L. Dittmar, Y. Liu, M. Liang, M. Kohli, S.N. Thibodeau, L. Boardman, L. Wang, Characterization of human plasma-derived exosomal RNAs by deep sequencing, BMC genomics, 14 (2013) 319.

[18] A. Eirin, S.M. Riester, X.Y. Zhu, H. Tang, J.M. Evans, D. O'Brien, A.J. van Wijnen, L.O. Lerman, MicroRNA and mRNA cargo of extracellular vesicles from porcine adipose tissue-derived mesenchymal stem cells, Gene, 551 (2014) 55-64.

[19] E.N. Nolte-'t Hoen, H.P. Buermans, M. Waasdorp, W. Stoorvogel, M.H. Wauben, P.A. t Hoen, Deep sequencing of RNA from immune cell-derived vesicles uncovers the selective incorporation of small non-coding RNA biotypes with potential regulatory functions, Nucleic Acids Res, 40 (2012) 9272-9285.

[20] K.C. Miranda, D.T. Bond, J.Z. Levin, X. Adiconis, A. Sivachenko, C. Russ, D. Brown, C. Nusbaum, L.M. Russo, Massively parallel sequencing of human urinary exosome/microvesicle RNA reveals a predominance of non-coding RNA, PloS one, 9 (2014) e96094.

[21] N. Guzman, K. Agarwal, D. Asthagiri, L. Yu, M. Saji, M.D. Ringel, M.E. Paulaitis, Breast Cancer-Specific miR Signature Unique to Extracellular Vesicles Includes "microRNA-like" tRNA Fragments, Molecular cancer research : MCR, 13 (2015) 891-901.

[22] J. Ratajczak, K. Miekus, M. Kucia, J. Zhang, R. Reca, P. Dvorak, M.Z. Ratajczak, Embryonic stem cell-derived microvesicles reprogram hematopoietic progenitors: evidence for horizontal transfer of mRNA and protein delivery, Leukemia, 20 (2006) 847-856.

[23] M. Baj-Krzyworzeka, R. Szatanek, K. Weglarczyk, J. Baran, B. Urbanowicz, P. Branski, M.Z. Ratajczak, M. Zembala, Tumour-derived microvesicles carry several surface determinants and mRNA of tumour cells and transfer some of these determinants to monocytes, Cancer Immunol Immunother, 55 (2006) 808-818.

[24] J. Skog, T. Wurdinger, S. van Rijn, D.H. Meijer, L. Gainche, M. Sena-Esteves, W.T. Curry, Jr., B.S. Carter, A.M. Krichevsky, X.O. Breakefield, Glioblastoma microvesicles transport RNA and proteins that promote tumour growth and provide diagnostic biomarkers, Nature cell biology, 10 (2008) 1470-1476.

[25] K. Ekstrom, H. Valadi, M. Sjostrand, C. Malmhall, A. Bossios, M. Eldh, J. Lotvall, Characterization of mRNA and microRNA in human mast cell-derived exosomes and their transfer to other mast cells and blood CD34 progenitor cells, Journal of extracellular vesicles, 1 (2012).

[26] S. Peng, X.S. Liu, S. Huang, Z. Li, H. Pan, W. Zhen, K.D. Luk, X.E. Guo, W.W. Lu, The cross-talk between osteoclasts and osteoblasts in response to strontium treatment: involvement of osteoprotegerin, Bone, 49 (2011) 1290-1298.

[27] S. Muruganandan, A.A. Roman, C.J. Sinal, Adipocyte differentiation of bone marrow-derived mesenchymal stem cells: cross talk with the osteoblastogenic program, Cell Mol Life Sci, 66 (2009) 236-253.

[28] L.M. Calvi, G.B. Adams, K.W. Weibrecht, J.M. Weber, D.P. Olson, M.C. Knight, R.P. Martin, E. Schipani, P. Divieti, F.R. Bringhurst, L.A. Milner, H.M. Kronenberg, D.T. Scadden, Osteoblastic cells regulate the haematopoietic stem cell niche, Nature, 425 (2003) 841-846.

[29] J. Morhayim, J. van de Peppel, J.A. Demmers, G. Kocer, A.L. Nigg, M. van Driel, H. Chiba, J.P. van Leeuwen, Proteomic signatures of extracellular vesicles secreted by nonmineralizing and mineralizing human osteoblasts and stimulation of tumor cell growth, FASEB journal : official publication of the Federation of American Societies for Experimental Biology, 29 (2015) 274-285.

[30] A. Dudakovic, E. Camilleri, S.M. Riester, E.A. Lewallen, S. Kvasha, X. Chen, D.J. Radel, J.M. Anderson, A.A. Nair, J.M. Evans, A.J. Krych, J. Smith, D.R. Deyle, J.L. Stein, G.S. Stein, H.J. Im, S.M. Cool, J.J. Westendorf, S. Kakar, A.B. Dietz, A.J. van Wijnen, High-resolution molecular validation of self-renewal and spontaneous

differentiation in clinical-grade adipose-tissue derived human mesenchymal stem cells, Journal of cellular biochemistry, 115 (2014) 1816-1828.

[31] W. Huang da, B.T. Sherman, R.A. Lempicki, Systematic and integrative analysis of large gene lists using DAVID bioinformatics resources, Nat Protoc, 4 (2009) 44-57.

[32] M. Pathan, S. Keerthikumar, C.S. Ang, L. Gangoda, C.Y. Quek, N.A. Williamson, D. Mouradov, O.M. Sieber, R.J. Simpson, A. Salim, A. Bacic, A.F. Hill, D.A. Stroud, M.T. Ryan, J.I. Agbinya, J.M. Mariadason, A.W. Burgess, S. Mathivanan, FunRich: An open access standalone functional enrichment and interaction network analysis tool, Proteomics, 15 (2015) 2597-2601.

[33] M. Eldh, J. Lotvall, C. Malmhall, K. Ekstrom, Importance of RNA isolation methods for analysis of exosomal RNA: evaluation of different methods, Molecular immunology, 50 (2012) 278-286.

[34] J. Van Deun, P. Mestdagh, R. Sormunen, V. Cocquyt, K. Vermaelen, J. Vandesompele, M. Bracke, O. De Wever, A. Hendrix, The impact of disparate isolation methods for extracellular vesicles on downstream RNA profiling, Journal of extracellular vesicles, 3 (2014).

[35] V. Palanisamy, S. Sharma, A. Deshpande, H. Zhou, J. Gimzewski, D.T. Wong, Nanostructural and transcriptomic analyses of human saliva derived exosomes, PloS one, 5 (2010) e8577.

[36] C. Lasser, V.S. Alikhani, K. Ekstrom, M. Eldh, P.T. Paredes, A. Bossios, M. Sjostrand, S. Gabrielsson, J. Lotvall, H. Valadi, Human saliva, plasma and breast milk exosomes contain RNA: uptake by macrophages, Journal of translational medicine, 9 (2011) 9.

[37] M. Kesimer, M. Scull, B. Brighton, G. DeMaria, K. Burns, W. O'Neal, R.J. Pickles, J.K. Sheehan, Characterization of exosome-like vesicles released from human tracheobronchial ciliated epithelium: a possible role in innate defense, FASEB journal : official publication of the Federation of American Societies for Experimental Biology, 23 (2009) 1858-1868.

[38] T. Ravasi, H. Suzuki, K.C. Pang, S. Katayama, M. Furuno, R. Okunishi, S. Fukuda, K. Ru, M.C. Frith, M.M. Gongora, S.M. Grimmond, D.A. Hume, Y. Hayashizaki, J.S. Mattick, Experimental validation of the regulated expression of large numbers of non-coding RNAs from the mouse genome, Genome research, 16 (2006) 11-19.

[39] A.O. Batagov, I.V. Kurochkin, Exosomes secreted by human cells transport largely mRNA fragments that are enriched in the 3'-untranslated regions, Biology direct, 8 (2013) 12.

[40] M.C. Deregibus, V. Cantaluppi, R. Calogero, M. Lo Iacono, C. Tetta, L. Biancone, S. Bruno, B. Bussolati, G. Camussi, Endothelial progenitor cell derived microvesicles activate an angiogenic program in endothelial cells by a horizontal transfer of mRNA, Blood, 110 (2007) 2440-2448.

[41] S. Bruno, C. Grange, M.C. Deregibus, R.A. Calogero, S. Saviozzi, F. Collino, L. Morando, A. Busca, M. Falda, B. Bussolati, C. Tetta, G. Camussi, Mesenchymal stem cell-derived microvesicles protect against acute tubular injury, J Am Soc Nephrol, 20 (2009) 1053-1067.

[42] A. Zomer, C. Maynard, F.J. Verweij, A. Kamermans, R. Schafer, E. Beerling, R.M. Schiffelers, E. de Wit, J. Berenguer, S.I. Ellenbroek, T. Wurdinger, D.M. Pegtel, J. van Rheenen, In Vivo imaging reveals extracellular vesicle-mediated phenocopying of metastatic behavior, Cell, 161 (2015) 1046-1057.

[43] M.W. Graner, O. Alzate, A.M. Dechkovskaia, J.D. Keene, J.H. Sampson, D.A. Mitchell, D.D. Bigner, Proteomic and immunologic analyses of brain tumor

exosomes, FASEB journal : official publication of the Federation of American Societies for Experimental Biology, 23 (2009) 1541-1557.

[44] P. Jenjaroenpun, Y. Kremenska, V.M. Nair, M. Kremenskoy, B. Joseph, I.V. Kurochkin, Characterization of RNA in exosomes secreted by human breast cancer cell lines using next-generation sequencing, PeerJ, 1 (2013) e201.

[45] A.H. Hutagalung, P.J. Novick, Role of Rab GTPases in membrane traffic and cell physiology, Physiological reviews, 91 (2011) 119-149.

[46] A.M. Marzesco, I. Dunia, R. Pandjaitan, M. Recouvreur, D. Dauzonne, E.L. Benedetti, D. Louvard, A. Zahraoui, The small GTPase Rab13 regulates assembly of functional tight junctions in epithelial cells, Mol Biol Cell, 13 (2002) 1819-1831.

[47] N. Nishimura, T. Sasaki, Rab family small G proteins in regulation of epithelial apical junctions, Frontiers in bioscience, 14 (2009) 2115-2129.

[48] F.P. Coxon, F.H. Ebetino, E.H. Mules, M.C. Seabra, C.E. McKenna, M.J. Rogers, Phosphonocarboxylate inhibitors of Rab geranylgeranyl transferase disrupt the prenylation and membrane localization of Rab proteins in osteoclasts in vitro and in vivo, Bone, 37 (2005) 349-358.

[49] N.J. Pavlos, J. Xu, D. Riedel, J.S. Yeoh, S.L. Teitelbaum, J.M. Papadimitriou, R. Jahn, F.P. Ross, M.H. Zheng, Rab3D regulates a novel vesicular trafficking pathway that is required for osteoclastic bone resorption, Molecular and cellular biology, 25 (2005) 5253-5269.

[50] M.J. Hirvonen, M.T. Mulari, K.G. Buki, P. Vihko, P.L. Harkonen, H.K. Vaananen, Rab13 is upregulated during osteoclast differentiation and associates with small vesicles revealing polarized distribution in resorbing cells, The journal of histochemistry and cytochemistry : official journal of the Histochemistry Society, 60 (2012) 537-549.

FIGURE CAPTIONS

Fig. 1. RNA profiling of human osteoblasts and osteoblast-EVs. (a-b) Representative Agilent 2100 Bioanalyzer electropherograms show the size distribution of total RNA extracted from (a) osteoblasts and (b) osteoblast-EVs (N = 3). Arrows show the characteristic cellular 18S (*left)* and 28S (r*ight*) rRNA peaks. FU, fluorescent units. s, seconds (time).

Fig. 2. Flowchart of the mRNA-sequencing data analysis. Total cellular and EV-RNA was isolated using TRIzol® extraction method, and after poly-A tail selection with oligo(dT) primers the RNA was sequenced via high throughput next-generation sequencing (N = 3). Initially, the reads were mapped to human genome and then the read counts were normalized and converted to counts per million mapped reads (CPM), which were subsequently converted to reads per kilobase per million (RPKM) mapped reads using Edge R. The reads were further filtered to remove low quality reads (CPM $\leq$ 1 and RPKM $\leq$ 0.1). Only the transcripts that mapped to mRNAs, which were detected in all replicates were considered for further analysis. Highly abundant mRNA transcripts that were enriched in EVs compared to the donor osteoblasts were studied via volcano plot and MA plot analyses.

Fig. 3. Next-generation sequencing mRNA profiling of osteoblast-EVs. (a) Scatter plot shows the correlation (R^2: 0.731) of normalized read counts (average CPM)

between cellular and EV transcripts (N = 3). (b) Pie chart shows the fraction of transcripts that were mapped to protein-coding mRNAs in EVs (91.80%, dark gray). Cellular mRNA percentage is shown in brackets. (c) Classification of the detected cellular and EV-mRNAs shows the fraction (%) of mRNAs that encode proteins involved in diverse biological functions determined by IPA analysis.

Fig. 4. The most abundant cellular and EV-mRNAs. (a) Venn diagram shows the distribution of mRNAs between osteoblasts and EVs. (b) Top 100 most abundant mRNAs make up more than 50% of the total RPKM values for EVs. (c) Top 100 EV-mRNAs are mostly annotated to genes encoding for proteins involved in protein synthesis and RNA processing. (d-e) RPKM values of the representative top 100 (d) EV-mRNAs (mean ± SD) (N = 3) and (e) cellular RNAs (mean ± SD) (N = 3).

Fig. 5. Selectively enriched EV-mRNAs. (a) Volcano plot (significance versus fold change) shows the significantly ($P < 0.05$, compared with osteoblasts by Student's *t*-test) abundant (≥ two-fold; 254 mRNAs; *right*) and depleted (≤ 0.5-fold; 2192 mRNAs; *left*) EV-mRNAs based on CPM values (N = 3). The top 10 most enriched EV-mRNAs are highlighted in blue. (b) Fold change distribution of selected genes annotated to overrepresented biological processes, such as induction of proliferation and expansion of hematopoietic stem and progenitor cells (HSPCs), recruitment of osteoclasts, and priming of adipocytes, identified by IPA (mean ± SD) (N = 3). (c) Venn diagram shows the number of unique mRNAs detected in osteoblast-EVs in

comparison with Vesiclepedia. (d) Venn diagram shows the overlap between the EV-protein and -mRNA content.

Fig. 6. Exon coverage of EV-mRNAs. (a) The number of EV-mRNAs and the corresponding fraction of exons that are covered with reads for a given mRNA compared to the cells. (b-e) The distribution of read counts (RPKM) across the different exons of selected enriched EV-mRNAs in EVs (black solid line) and cells (gray dotted line) (mean ± SD) (N = 3). f) Length (bp; base pairs) distribution of full-length (100% exon coverage) enriched EV-mRNAs.

Fig. 7. EVs are selectively enriched with *RAB13* mRNA. (a) MA plot (fold change versus abundance) shows the RPKM values of the significantly enriched EV-mRNAs. *RAB13* is both the most enriched and abundant mRNA detected in EVs.(b) MA plot of the Rab family mRNAs detected in both cells and EVs. *RAB13* is the only Rab family mRNA that is highly enriched in EVs compared to the donor osteoblasts. (c-d) Relative expressions of *RAB13* and *ATP5E* in EVs and cells by (c) mRNA-sequencing (mean ± SD) (N = 3) and (d) qPCR (mean ± SD) (N = 6). The mRNA-sequencing results are shown as average fold change of RPKM values relative to *GAPDH*. The qPCR results are normalized to average *GAPDH* expression. (e) IPA interaction network shows the predicted biological functions (gray) associated with the downstream targets (black) of RAB13 protein. * $P < 0.05$, compared with cells by Student's *t*-test; ns, not significant.

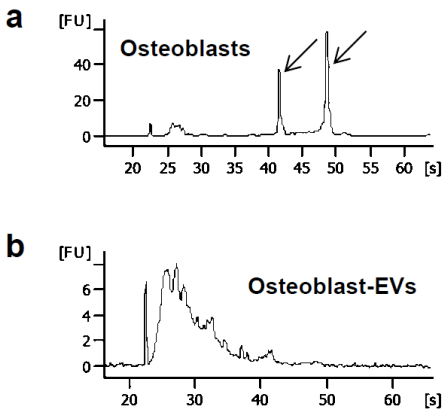

Figure 1

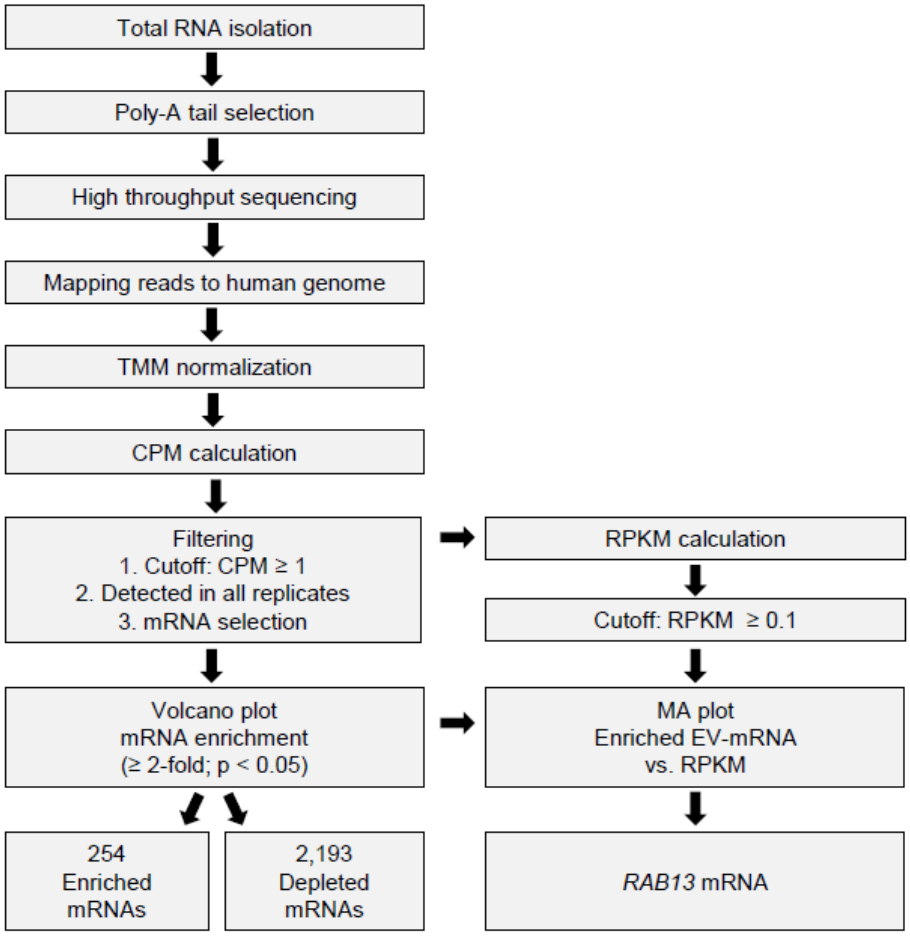

Figure 2

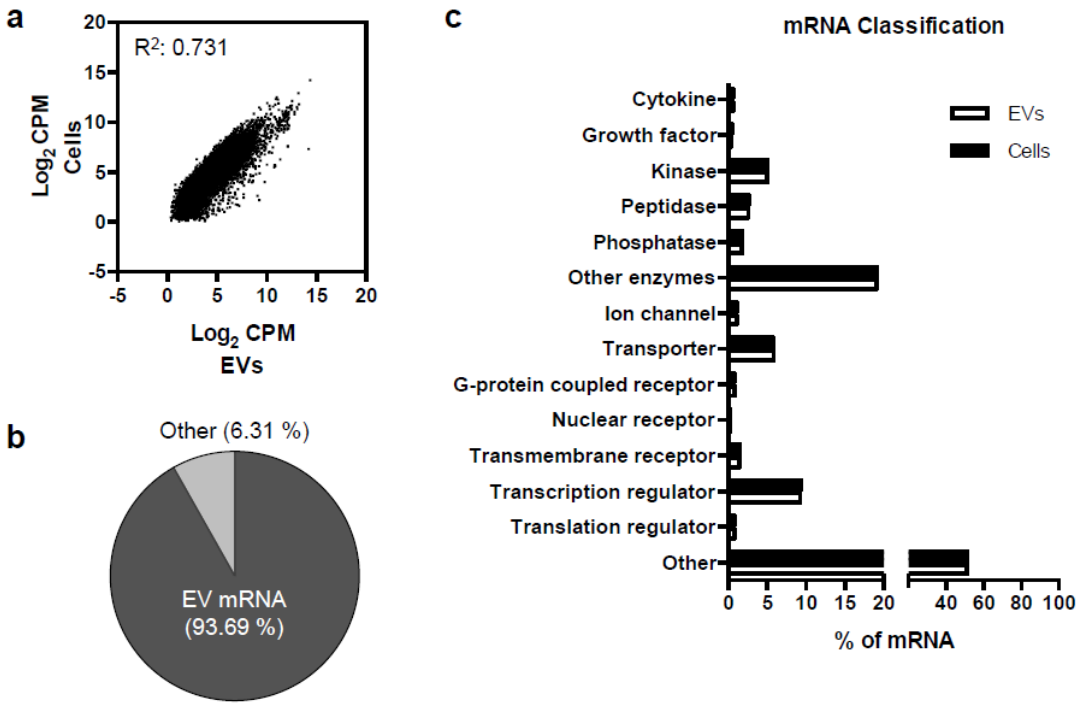

Figure 3

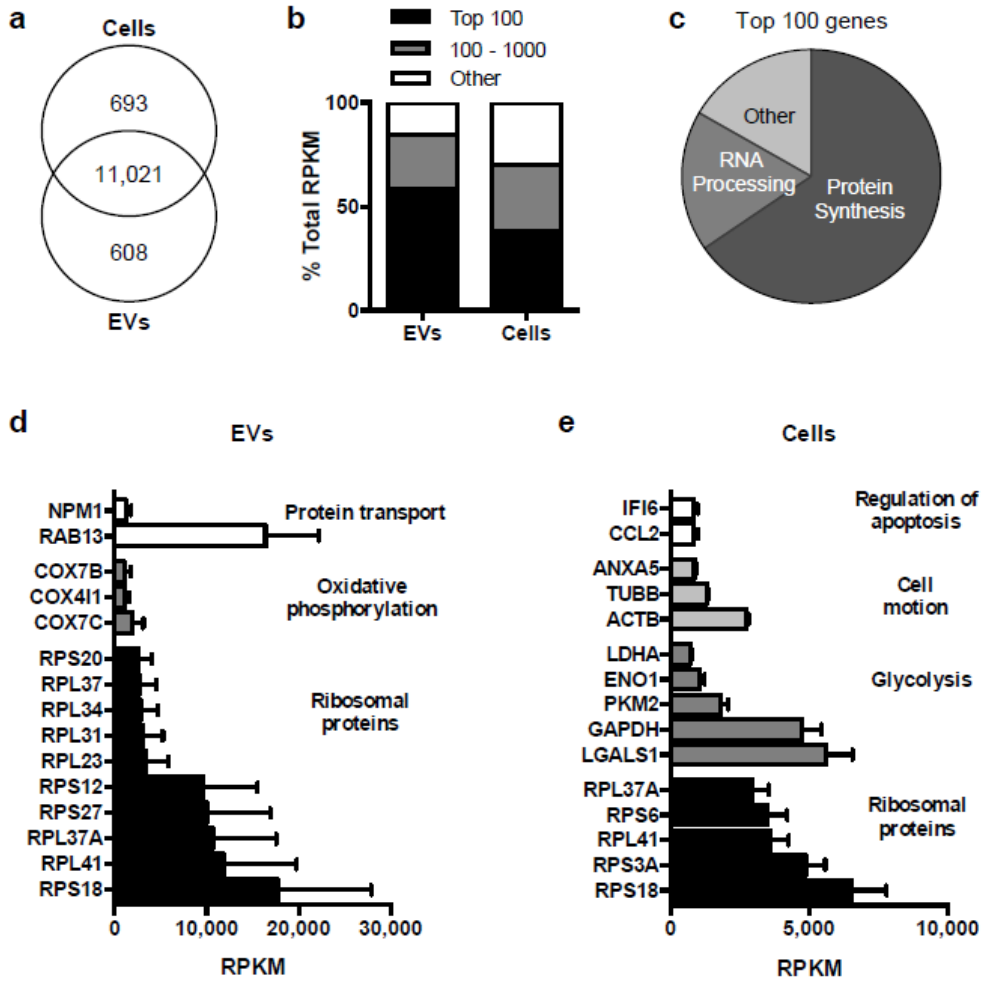

Figure 4

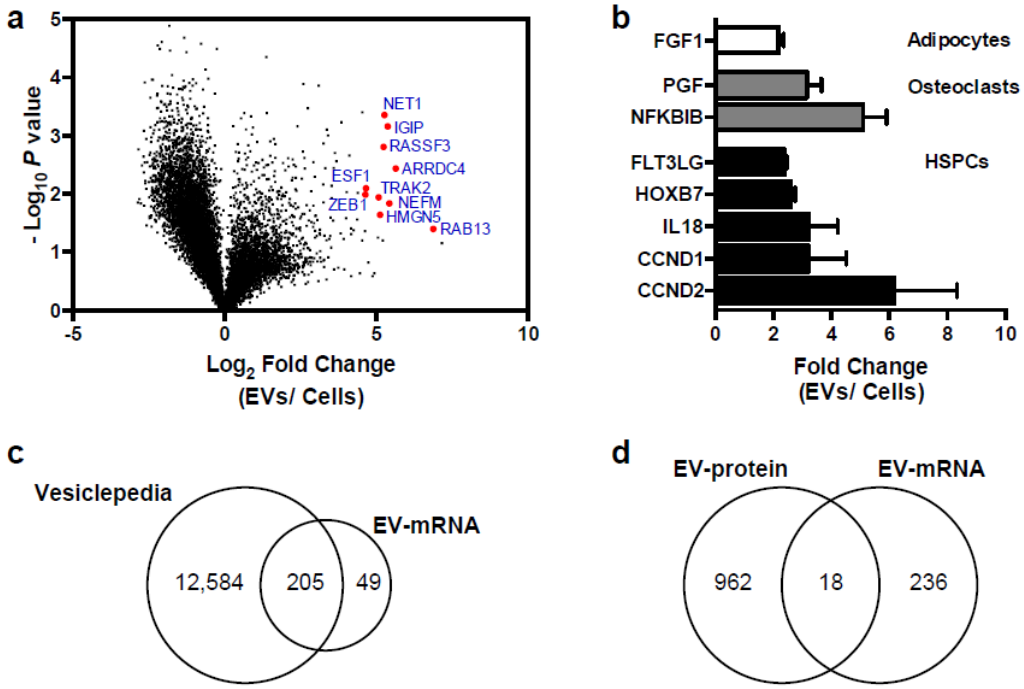

Figure 5

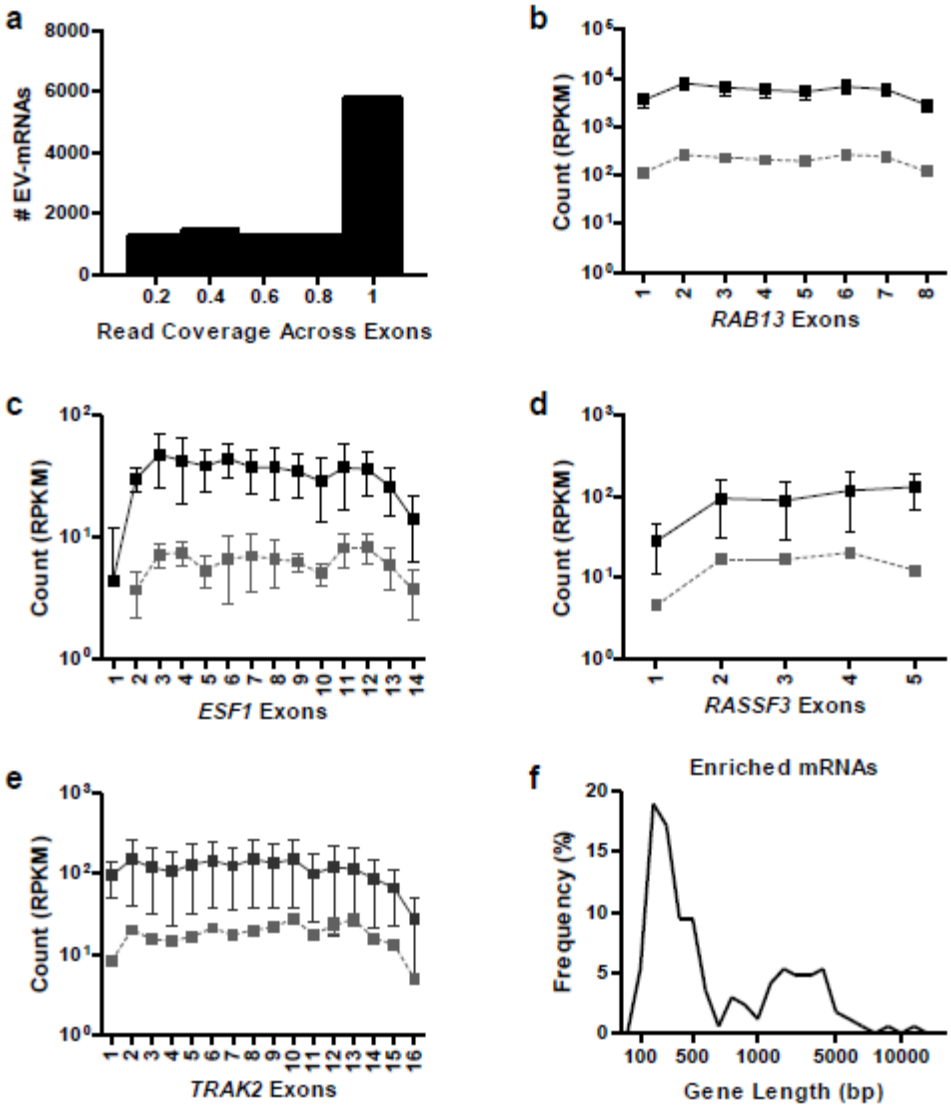

Figure 6

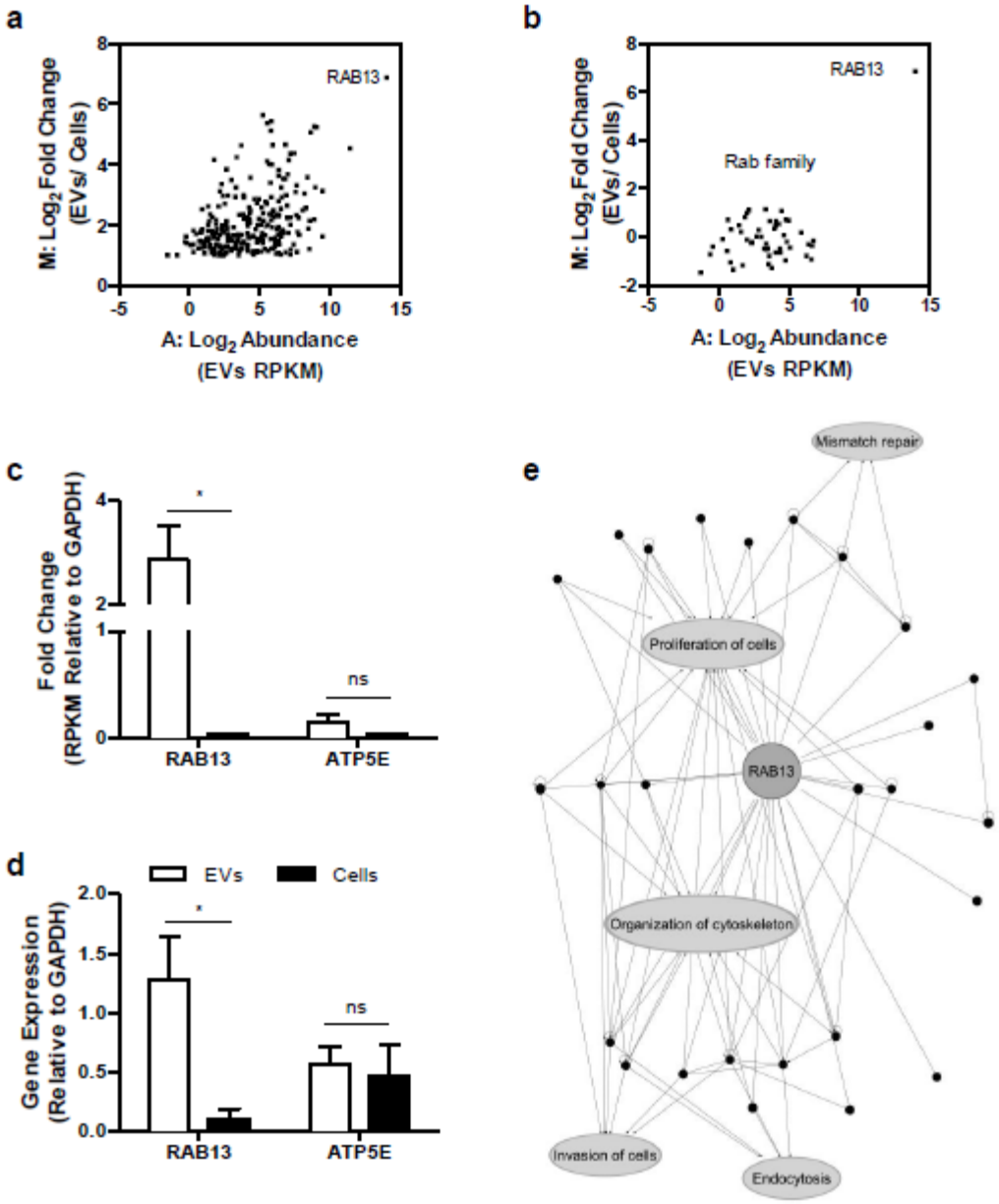

Figure 7

Highlights

- Osteoblasts secrete nano-sized EVs packaged with regulatory mRNA
- Global expression profiles of parental cells and EVs confirm selective mRNA sorting
- EVs are specifically depleted of mRNAs essential for basic cellular activities
- Overrepresented EV-mRNAs are associated with protein translation and RNA processing